



Contents lists available at ScienceDirect

Deep-Sea Research II

journal homepage: www.elsevier.com/locate/dsr2

Changes in source waters to the Southern California Bight

Steven J. Bograd^{a,*}, Mercedes Pozo Buil^b, Emanuele Di Lorenzo^b, Carmen G. Castro^c, Isaac D. Schroeder^a, Ralf Goericke^d, Clarissa R. Anderson^e, Claudia Benitez-Nelson^f, Frank A. Whitney^g

^a NOAA, Southwest Fisheries Science Center, Environmental Research Division, 1352 Lighthouse Avenue, Pacific Grove, CA 93950-2097, USA

^b School of Earth and Atmospheric Sciences, Georgia Institute of Technology, Atlanta, GA 30332, USA

^c Instituto de Investigaciones Marinas, Consejo Superior de Investigaciones Científicas, Vigo, Spain

^d Integrative Oceanography Division, Scripps Institution of Oceanography, La Jolla, CA 92093, USA

^e Institute of Marine Sciences, University of California, Santa Cruz, Santa Cruz, CA 95064, USA

^f Department of Earth and Ocean Sciences and Marine Science Program, University of South Carolina, Columbia, SC 29208, USA

^g Fisheries and Oceans Canada, Institute of Ocean Sciences, Sidney, BC, Canada V8L 4B2

ARTICLE INFO

Keywords:

California Current System
California Undercurrent
CalCOFI
Dissolved oxygen
Inorganic nutrients
Water masses
Upwelling

ABSTRACT

Historical hydrographic data (1984–2012) from the California Cooperative Oceanic Fisheries Investigations (CalCOFI) program and global reanalysis products were used to quantify recent water mass variability off the coast of Southern California. Dissolved oxygen concentrations continued to decline within the lower pycnocline, concurrent with strong increases in nitrate and phosphate that have spatial patterns matching those of dissolved oxygen. Silicic acid also shows an increasing trend in the offshore portion of the region, but has strong and opposing trends in the upper (increasing) and lower-pycnocline (decreasing) within the Southern California Bight. The varying rates of change in the inorganic nutrients yield a more complex pattern of variability in the nutrient ratios, resulting in large decreases in the N:P and Si:N ratios within the Southern California Bight at depths that provide source waters for upwelling. Basin-scale reanalysis products are consistent with low-frequency water mass changes observed off Southern California and suggest that advection of modified source waters is the cause of the variability. The biogeochemical changes described here may have important impacts on the regional ecosystem, including a reduction of viable pelagic habitat and community reorganization.

Published by Elsevier Ltd. This is an open access article under the CC BY-NC-ND license (<http://creativecommons.org/licenses/by-nc-nd/3.0/>).

1. Introduction

Recent studies have demonstrated widespread impacts of climate change on marine ecosystems, including changes in species abundance, distribution and demography, community reorganization, phenological shifts, and ocean acidification (Doney et al., 2012; Poloczanska et al., 2013; Bernhardt and Leslie, 2013 and references within). Many of the observed rates of change in marine systems are comparable to, or greater than, those observed in terrestrial systems (Burrows et al., 2011; Poloczanska et al., 2013). Changes in ocean biogeochemistry are among the most significant in terms of their potential impacts on marine life, particularly in coastal ecosystems (Doney et al., 2009; Hauri et al., 2009; Keeling et al., 2010; Gruber 2011; Gruber et al., 2012; Taylor et al., 2012).

Models forced by increasing greenhouse gases predict a decline in midwater oceanic dissolved oxygen (DO) as a result of enhanced stratification and reduced ventilation (Sarmiento et al., 1998; Keeling and Garcia, 2002). Analyses of long-term oceanic datasets have revealed declining DO levels that are consistent with these climate projections (Deutsch et al., 2005, 2011; Whitney et al., 2007, 2013). In the equatorial Pacific, Stramma et al. (2008, 2010) have shown a thickening and shoaling of the Oxygen Minimum Zone (OMZ), which could result in reduced oxygen supply to the boundary upwelling systems of North and South America. In the Southern California Current, DO declines of 1–2 $\mu\text{mol kg}^{-1} \text{y}^{-1}$ have been observed in recent years (Bograd et al., 2008; McClatchie et al., 2010; Meinvielle and Johnson, 2013), while the frequency of hypoxic events has increased in the northern California Current (Chan et al., 2008; Booth et al., 2012). It is expected that changes in other key water properties will also occur, including the inorganic nutrient concentrations that drive ocean productivity (Whitney et al., 2013). Shoaling of the OMZ will likely lead to significant and complex ecological changes including

* Corresponding author. Tel.: +1 831 648 8314.

E-mail address: steven.bograd@noaa.gov (S.J. Bograd).

anoxia for benthic organisms, reduction in pelagic habitat for top predators (Koslow et al., 2011), and more numerous invasions from hypoxia tolerant species (Stewart et al., 2012). Alterations in total nutrient concentrations, or the relative content of the nutrients, could lead to community reorganization within marine ecosystems (Margalef, 1962, 1978; Smayda, 1963; Karl et al., 2012; Taylor et al., 2012).

While a number of studies have investigated long-term oxygen dynamics throughout the tropical and extratropical Pacific, fewer studies have reported on long-term variability in nutrient content. This is largely due to a lack of nutrient time series of sufficient length to detect low-frequency climate signals. A long data record within the Oyashio, off the northern coast of Japan, has shown a freshening of the winter mixed layer and declining phosphate levels (Ono et al., 2001). Over a broader region of the subarctic Pacific, Ono et al. (2008) reported declines in summer near-surface nutrient levels over the period 1975–2005, accompanied by increases (decreases) in intermediate layer nutrients (oxygen) (Watanabe et al., 2008). At the long time series Station 'P' in the northeast Pacific, Whitney (2011) found weak increasing trends in surface layer nutrient concentrations, even though increased stratification (Freeland et al., 1997) is expected to reduce the winter resupply of mixed layer nutrients. Whitney et al. (2013) synthesized these and other observations from several time series programs throughout the North Pacific to document a long-term enrichment of subarctic pycnocline nitrate (200 Gmol y^{-1}). They suggested that this enrichment counters the effects of increased stratification, resulting in a surface nutrient supply that remains nearly constant. Di Lorenzo et al. (2009) further suggested that decadal oscillations in upper ocean nutrients in the eastern North Pacific results from atmospherically-driven changes in the strength of the North Pacific gyres.

The California Current Ecosystem (CCE) Long Term Ecological Research (LTER) site is within a productive coastal upwelling biome that is strongly influenced by remote and local physical forcing. The site is built upon more than 65 years of extensive sampling of the regional physics, chemistry, and biology, through the California Cooperative Oceanic Fisheries Investigations (CalCOFI) program (Hewitt, 1988; Peña and Bograd, 2007). The long CalCOFI time series provide a unique opportunity to investigate climate impacts on the CCE, including changes in regional biogeochemistry and the mechanisms leading to transitions between ecosystem states. Here we use the CalCOFI dataset to investigate long-term alteration of water mass characteristics in the CCE-LTER region, focusing on inorganic nutrient concentrations, and speculate on the mechanisms and biological implications of these changes.

2. Data and methods

2.1. CalCOFI time series

Since 1984, CalCOFI has consistently sampled six nominal lines in the southern CCE from San Diego to Pt. Conception quarterly, with target months of January, April, July, and October (Fig. 1A), with measurements of inorganic nutrients and chlorophyll. Prior to 1984, only basic hydrographic variables and dissolved oxygen were routinely measured. Stations are designated by a line and station number, with nominal station spacing of $\sim 70 \text{ km}$ offshore but considerably less inshore of the islands. Routine station occupations (on 66 standard stations) deploy a SeaBird CTD instrument with a 24-place rosette, which is equipped with 24 10-L plastic (PVC) Niskin bottles (Scripps Institution of Oceanography, 2012). Casts are typically made to $\sim 525 \text{ m}$ depth, bottom depth permitting, with continuous measurements of pressure, temperature, conductivity, dissolved oxygen and chlorophyll fluorescence. Bottle samples are taken at 20 depths, and are generally chosen to provide high resolution ($< 10 \text{ m}$) around the subsurface chlorophyll maximum and the shallow salinity minimum of the upper thermocline. Salinity, dissolved oxygen and inorganic nutrients are determined for all depths sampled, while chlorophyll-*a* and phaeopigments are determined within the upper 200 m, bottom depth permitting. Pressures and temperatures for each water sample were derived from the CTD signals recorded just prior to *in situ* bottle sampling. Salinities were analyzed at sea from the bottle data using a Guildline model 8410 Portasal salinometer, with results quality controlled using discrete measurements from the Niskins (Scripps Institution of Oceanography, 2012). There have been more than 6700 station occupations on the CalCOFI grid off southern California between January 1984 and April 2012. CalCOFI's longevity and consistent sampling methodology allow for reliable time series analyses at a number of geographically fixed locations within the southern CCE.

Dissolved oxygen samples were collected in calibrated 100 mL iodine flasks and analyzed at sea by the modified Winkler method (Carpenter, 1965), using the equipment and procedure outlined by Anderson (1971). Percent oxygen saturation was calculated from the equations of Garcia and Gordon (1992). Dissolved silicic acid, phosphate, nitrate and nitrite concentrations were determined at sea using an automated analyzer (Atlas et al., 1971), following procedures similar to those described in Gordon et al. (1993). Estimates of precision of these standard techniques are $0.001 \text{ }^\circ\text{C}$, 0.002 for salinity, 0.02 mL L^{-1} for DO, and 0.5 , 0.01 , and $0.1 \text{ } \mu\text{mol kg}^{-1}$ for silicic acid, phosphate, and nitrate, respectively (Scripps Institution of Oceanography, 2012). Further details of the standard sampling and

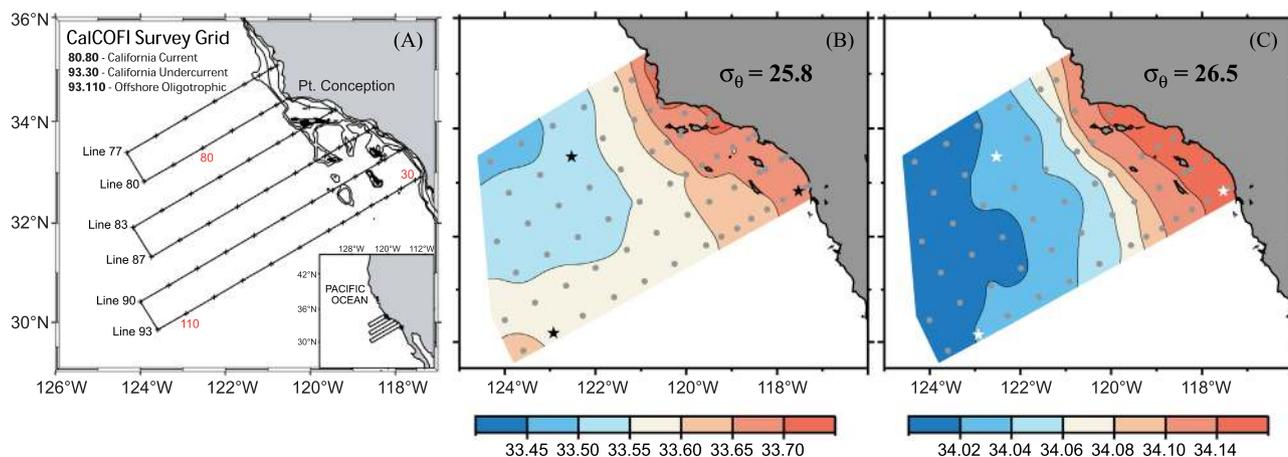


Fig. 1. (A) Nominal CalCOFI grid showing Lines and Stations. Mean salinity on the (B) $\sigma_\theta = 25.8 \text{ kg m}^{-3}$ and (C) $\sigma_\theta = 26.5 \text{ kg m}^{-3}$ isopycnal surfaces. Locations of Stations 80.80, 93.30 and 93.110 are marked with stars and all other stations with gray dots. CalCOFI salinity climatologies are for the 1984–2012 period.

analysis procedures, along with all data and derived variables, can be found in any of the CalCOFI data reports (e.g., [Scripps Institution of Oceanography, 2012](#)) or online at www.calcofi.org.

In addition to the variables described above, we also derive spiciness, a state variable (units of σ_t) that is most sensitive to isopycnal thermohaline variations and least correlated with the density field ([Flament, 2002](#); [Bograd and Lynn, 2003](#)). Spiciness is conserved in isentropic motions, and its value increases with increasing temperature and salinity. As density-compensated temperature and salinity variations along isopycnal surfaces, spiciness anomalies have been used as a tracer of basin-scale water mass movements ([Schneider, 2000](#); [Sasaki et al., 2010](#); [Li et al., 2012](#)).

2.2. Focal regions

Here we focus on long-term linear trends in water column physical and chemical properties at select stations and isopycnal levels that represent the dominant source waters to the region ([Fig. 1](#)): Station 80.80 (33° 28.8'N, 122° 31.8'W) is located ~220 km offshore of Pt. Conception, typically within the main core of the California Current; Station 93.30 (32° 51.0'N, 117° 31.8'W) is located over the continental slope within the Southern California Bight (SCB) and is strongly impacted by the California Undercurrent ([Lynn and Simpson, 1987](#); [Lynn and Simpson, 1990](#)); Station 93.110 (30° 10.8'N, 122° 55.2'W) is located more than 600 km offshore of southern California, and represents water masses offshore of the main California Current core, within the oligotrophic North Pacific Subtropical Gyre (NPSG). We computed linear trends in water mass properties (isopycnal depth, spiciness, dissolved oxygen, inorganic nutrients and nutrient ratios) over the entire 28-year record (1984–2012), and also separately for each quarter (January–March, etc.). The magnitude of the linear trends were used to quantify the variability in each property over the record and to describe the three-dimensional spatial patterns of that variability. The short length of the time series precludes us from distinguishing secular trends (possibly driven by uni-directional climate change) from low-frequency climate variability.

2.3. Ocean reanalysis products

To identify potential mechanisms and time scales of the observed water mass variability, we further investigated long-term subsurface dynamics in the North Pacific using two global reanalysis products: the European Centre for Medium-range Weather Forecasting (ECMWF) Ocean Reanalysis System (ORA-S3) and the Simple Ocean Data Assimilation (SODA 2.1.6). ORA-S3 is based on the Hamburg Ocean Primitive Equation model ([Wolff et al., 1997](#)) and the optimal interpolation assimilation scheme (HOPE-OI scheme). This dataset covers the global ocean with a uniform 1° × 1° horizontal resolution and 29 levels in the vertical, spanning the period January 1959 to December 2009 ([Balmaseda et al., 2008](#)). The SODA reanalysis dataset is based on multivariate optimal interpolation using the Parallel Ocean Program POP 1.4 model ([Smith et al., 1992](#)). The spatial resolution of the SODA output is 0.5° × 0.5° in longitudinal and latitudinal directions and 40 vertical levels, spanning the period January 1958 to December 2008 ([Carton and Giese, 2008](#)). These two reanalysis products are available on Asia-Pacific Data-Research Center (APDRC), University of Hawaii (http://apdrc.soest.hawaii.edu/dods/public_data/Reanalysis_Data/ORA-S3/1x1_grid.info) and http://apdrc.soest.hawaii.edu/dods/public_data/SODA/soda_pop2.1.6.info.

3. Variability in water masses

The LTER-CCE/CalCOFI region has long been identified as a confluence of water mass influences from the subarctic Pacific, via

the California Current (CC), and from the northeastern tropical Pacific, via the California Undercurrent (CUC) ([Hickey, 1979, 1998](#); [Lynn and Simpson, 1987](#)). Their influences are evident in maps of the mean (1984–2012) properties on isopycnal surfaces ([Fig. 1](#)). The $\sigma_\theta=25.8 \text{ kg m}^{-3}$ isopycnal surface is located in the lower pycnocline, within the spiciness minimum zone. The low-salinity tongue offshore identifies the shallow (upper 200 m), equatorward flowing CC, which supplies the region with relatively cool, fresh (low spiciness) waters originating in the subarctic Pacific ([Lynn and Simpson, 1987](#)). The higher salinities on the shelf reflect upwelled waters ([Fig. 1B](#)). In the long-term mean, the core of the CC is located near Station 80.80 ([Lynn et al., 1982](#)), although the position of the core varies seasonally, moving closer to shore in spring–summer similar to that found by [Lynn et al. \(2003\)](#). The $\sigma_\theta=26.5 \text{ kg m}^{-3}$ isopycnal surface is at the depth of the subsurface spiciness maximum associated with the CUC, a poleward flow confined to the continental slope of the North American continental shelf that supplies the region with waters of tropical origin ([Reid, 1962, 1963](#); [Wooster and Reid, 1963](#); [Wooster and Jones, 1970](#); [Lynn and Simpson, 1987](#); [Pierce et al., 2000](#); [Castro et al., 2001](#); [Bograd and Lynn, 2003](#)) ([Fig. 1C](#)). The relatively warm and salty (high spiciness) waters brought into the region at this density surface spread offshore ([Lynn and Simpson, 1990](#)) and are often entrained within offshore-propagating mesoscale eddies ([Simpson and Lynn, 1990](#)). Station 93.30 is situated within the CUC core. Long-term changes in the physical and chemical properties observed at the stations identified above are therefore hypothesized to be indicative of large-scale changes in the volume and/or properties of source waters to the region.

3.1. Time series at source water stations

Water property time series on the $\sigma_\theta=25.8 \text{ kg m}^{-3}$ isopycnal surface at Station 80.80 and on the $\sigma_\theta=26.5 \text{ kg m}^{-3}$ isopycnal surface at Stations 93.30 and 93.110 reveal significant seasonal and interannual variability and long-term trends ([Fig. 2](#) and [Tables 1 and 2](#)). Both isopycnal surfaces rise in summer and fall in winter, but there is considerable interannual variability in their depths, the annual ranges of those depths, and the overall thickness of the water column between these two surfaces at any given station (not shown). There is no significant long-term trend in the depth of these surfaces at the CC (80.80) or CUC (93.30) stations ([Fig. 2](#)), but there is a significant positive trend in the depth of the $\sigma_\theta=26.5 \text{ kg m}^{-3}$ isopycnal surface at the offshore oligotrophic station (93.110), i.e. a shoaling of ~22 m over the 28-year period. El Niño events stand out as times of depressed isopycnals, primarily due to significant warming in the upper water column ([Bograd and Lynn, 2001](#); [Lynn and Bograd, 2002](#)).

Dissolved oxygen shows a long-term decline only at the deeper density level, reflecting a broad decline at mid to lower pycnocline depths throughout the North Pacific basin ([Fig. 2](#) and [Whitney et al., 2013](#)). The magnitude of the trend is strongest at the offshore station. These trends have been described in detail elsewhere ([Bograd et al., 2008](#); [McClatchie et al., 2010](#); [Whitney, 2011](#); [Whitney et al., 2013](#); [Meinvielle and Johnson, 2013](#)), and have been shown to influence the regional ecosystem through, for example, vertical compression of viable habitat for mesopelagic fishes ([Koslow et al., 2011](#)).

It is expected that nutrient content would change concomitantly with dissolved oxygen, since oxygen is consumed during the remineralization of marine detritus and release of dissolved nutrients ([Whitney et al., 2013](#)). Trends in the inorganic nutrients are apparent, although with significant heterogeneity between stations, depths and properties. At the CC station/depth (80.80, $\sigma_\theta=25.8 \text{ kg m}^{-3}$), interannual variability includes an extended period of relatively high nutrient content (and low DO) during

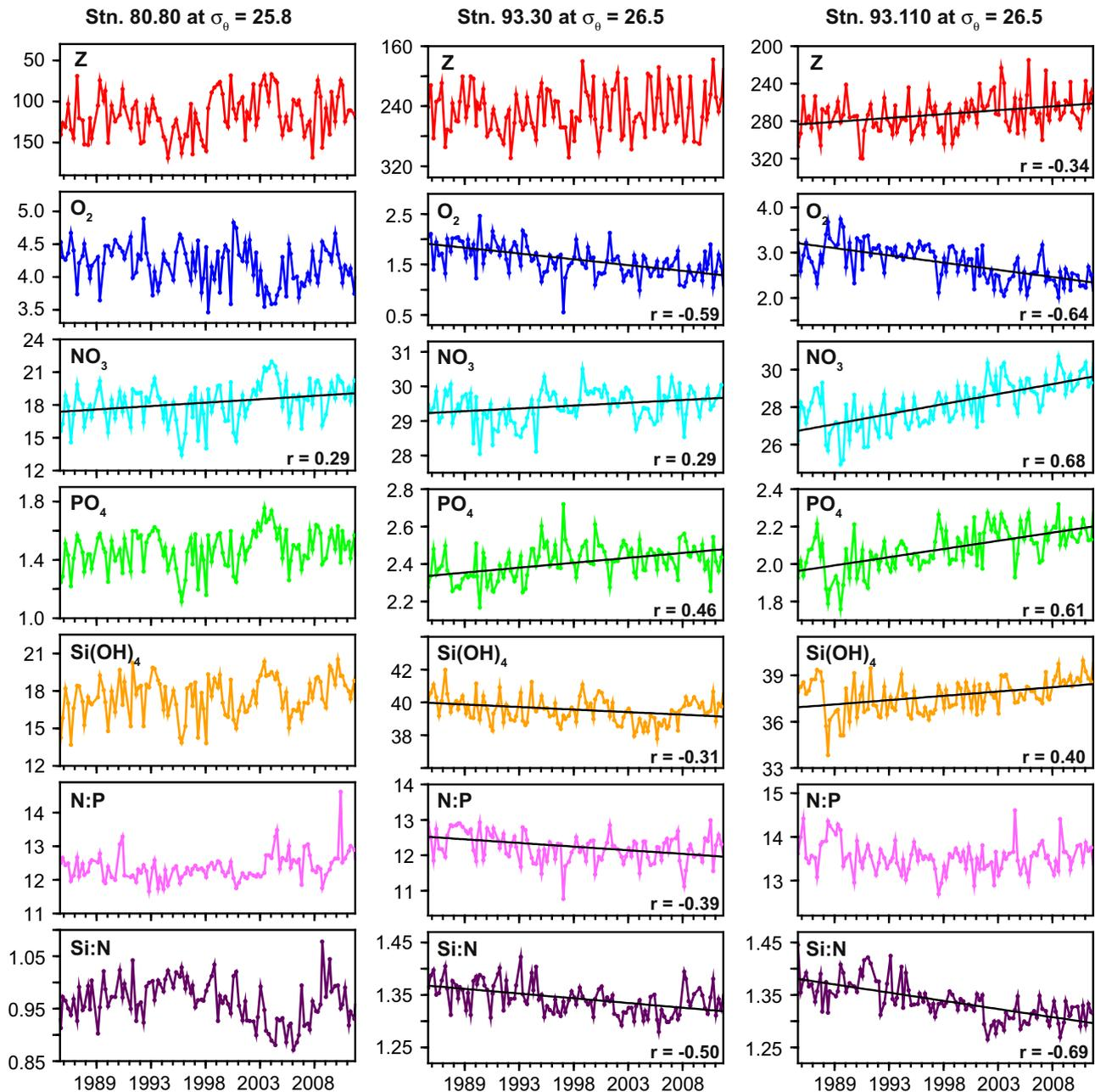


Fig. 2. Water property time series at Station 80.80 on the $\sigma_{\theta}=25.8 \text{ kg m}^{-3}$ isopycnal surface (left panels), Station 93.30 on the $\sigma_{\theta}=26.5 \text{ kg m}^{-3}$ isopycnal surface (middle panels), and Station 93.110 on the $\sigma_{\theta}=26.5 \text{ kg m}^{-3}$ isopycnal surface (right panels). From top to bottom, isopycnal depth (m), dissolved oxygen (mL L^{-1}), nitrate ($\mu\text{mol kg}^{-1}$), phosphate ($\mu\text{mol kg}^{-1}$), silicic acid ($\mu\text{mol kg}^{-1}$), nitrate:phosphate ratio, and silicic acid: nitrate ratio. Significant linear regressions ($p < 0.001$) are shown with black lines. Time series cover the period 1984–2012.

the years 2002 and 2005 (Fig. 2, left panels). There is a small but significant trend towards higher nitrate but no trend in the concentrations of phosphate or silicic acid, or in any of the nutrient ratios.

At the depth of the subsurface spiciness maximum ($\sigma_{\theta}=26.5 \text{ kg m}^{-3}$), there is a clear difference in the long-term variability in nutrient content between the waters within the SCB and those well offshore (Fig. 2, middle and right panels). At the CUC station (93.30), both nitrate and phosphate show significant long-term increases, while silicic acid shows a significant long-term decrease. Although both nitrate and phosphate increased over the period, their increase was at different rates, resulting in a substantial long-term decline in the N:P ratio. There is also a significant decrease in the Si:N ratio within the CUC core, reflecting the differential trends in these nutrients. Time-longitude plots of the Si:N ratio within

the lower pycnocline (not shown) reveal a regime-like shift across Line 93, with consistently higher values prior to 1995 and lower values after 2000. The long-term trends in nutrients are substantially larger at the offshore station (93.110) and, for silicic acid, in the opposite direction (Fig. 2, right panels). The relative rates of change also vary, resulting in no trend in the N:P ratio, but a significant negative trend in the Si:N ratio due to the strong increase in nitrate. The largest trend for any of the nutrient series was in the nitrate concentration at the offshore station (93.110) on the $\sigma_{\theta}=26.5 \text{ kg m}^{-3}$ isopycnal surface ($0.10 \mu\text{mol kg}^{-1} \text{ y}^{-1}$).

Linear trends derived separately for each quarter reveal seasonal differences that likely reflect the seasonal cycle of the regional circulation (Tables 1 and 2). The CC undergoes a seasonal progression from a single core positioned $\sim 300 \text{ km}$ offshore in winter to two cores approximately 300 km and $< 100 \text{ km}$ offshore in

Table 1

Annual and seasonal mean water property trends (change in variable per year; z , $m\ y^{-1}$; O_2 , $mL\ L^{-1}\ y^{-1}$; NO_3 , PO_4 , $Si(OH)_4$, $\mu mol\ kg^{-1}\ y^{-1}$) for CalCOFI Station 93.30 over the period 1984–2012. The top number is the magnitude of the trend on the $\sigma_\theta=25.8\ kg\ m^{-3}$ isopycnal surface and the bottom number is the magnitude of the trend on the $\sigma_\theta=26.5\ kg\ m^{-3}$ isopycnal surface. Trends that are not significant ($p > 0.05$) are shaded gray.

| | Annual | Winter | Spring | Summer | Fall |
|------------|------------------|------------------|------------------|------------------|------------------|
| z | –0.646 –0.312 | –0.745 –0.425 | –0.608 –0.501 | –0.858 –1.263 | –0.900 0.740 |
| O_2 | –0.017 –0.023 | –0.021 –0.025 | –0.009 –0.031 | –0.005 –0.016 | –0.029 –0.025 |
| NO_3 | 0.087 0.016 | 0.106 0.020 | 0.057 0.030 | 0.071 0.005 | 0.102 0.012 |
| PO_4 | 0.008 0.005 | 0.009 0.005 | 0.006 0.008 | 0.005 0.004 | 0.011 0.006 |
| $Si(OH)_4$ | 0.058 –0.031 | 0.085 –0.017 | 0.011 –0.035 | 0.016 –0.051 | 0.096 –0.019 |
| N:P | –0.005 –0.021 | 0.002 –0.020 | –0.009 –0.027 | 0.007 –0.019 | –0.021 –0.024 |
| Si:N | –0.002 –0.002 | –0.001 –0.002 | –0.002 –0.003 | –0.003 –0.002 | 0 –0.001 |

Table 2

Annual and seasonal mean water property trends (change in variable per year; z , $m\ y^{-1}$; O_2 , $mL\ L^{-1}\ y^{-1}$; NO_3 , PO_4 , $Si(OH)_4$, $\mu mol\ kg^{-1}\ y^{-1}$) for CalCOFI Station 93.110 over the period 1984–2012. The top number is the magnitude of the trend on the $\sigma_\theta=25.8\ kg\ m^{-3}$ isopycnal surface and the bottom number is the magnitude of the trend on the $\sigma_\theta=26.5\ kg\ m^{-3}$ isopycnal surface. Trends that are not significant ($p > 0.05$) are shaded gray.

| | Annual | Winter | Spring | Summer | Fall |
|------------|------------------|------------------|------------------|------------------|------------------|
| z | –0.761 –0.821 | –1.03 –1.274 | –0.709 –0.644 | –0.309 –0.225 | –0.929 –0.948 |
| O_2 | –0.009 –0.032 | –0.011 –0.039 | 0 –0.017 | –0.011 –0.031 | –0.014 –0.033 |
| NO_3 | 0.123 0.107 | 0.146 0.132 | 0.029 0.062 | 0.108 0.103 | 0.189 0.107 |
| PO_4 | 0.008 0.009 | 0.008 0.01 | 0.003 0.006 | 0.008 0.01 | 0.012 0.009 |
| $Si(OH)_4$ | 0.087 0.056 | 0.099 0.061 | 0.014 0.029 | 0.078 0.052 | 0.149 0.07 |
| N:P | 0.018 –0.006 | 0.031 –0.003 | –0.004 –0.006 | 0.003 –0.013 | 0.032 –0.006 |
| Si:N | –0.002 –0.003 | –0.003 –0.004 | –0.001 –0.002 | –0.002 –0.003 | –0.002 –0.003 |

spring/summer, as an upwelling jet develops nearshore (Lynn et al., 1982; Chelton, 1984; Lynn and Simpson, 1987; Lynn et al., 2003). This offshore current core strengthens in summer and autumn when its mean speeds and volume transports are highest (Lynn et al., 1982; Lynn and Simpson, 1987). The CUC also has its highest volume transports in summer and autumn (Lynn and Simpson, 1987). Additionally, geostrophically induced upwelling and winter convection have been shown to be important mechanisms for seasonal nutricline shoaling and the injection of nutrients into the euphotic zone (Mantyla et al., 2008). On the $\sigma_\theta=25.8\ kg\ m^{-3}$ isopycnal surface, the annual spatial patterns of dissolved oxygen and nutrient trends are most similar to the late-winter (January–March) patterns, when the largest trends occur, while the fewest significant trends occur in spring (April–June). These seasonal differences are most apparent in the offshore region (Table 2). The impact of CUC transport on the water property trends is evident in the seasonal trends on the $\sigma_\theta=26.5\ kg\ m^{-3}$ isopycnal surface (maps not shown). While there are significant water property trends at most stations in all seasons, the late summer (July–September) positive nitrate and phosphate trends are lowest, and negative silicic acid trend highest, at Station 93.30 (Table 1). This is consistent with a seasonal increase in CUC transport of

low-nutrient waters of subtropical origin (Castro et al., 2001; Meinville and Johnson, 2013).

3.2. Spatial patterns of water property trends

Maps of water property trends on the two isopycnal surfaces provide a broader view of water mass variability in the LTER-CCE/CalCOFI region (Fig. 3). The declines in DO are observed throughout the region, but are considerably stronger on the $\sigma_\theta=26.5\ kg\ m^{-3}$ isopycnal surface and on the offshore portion of the grid (Fig. 3), as has been described earlier (Bograd et al., 2008). The spatial patterns of trends in nitrate and phosphate are similar at both density levels: at $\sigma_\theta=25.8\ kg\ m^{-3}$, the largest trends are on the southern end of the grid, with the region around the mean CC core having weaker, though still significant, trends. On the $\sigma_\theta=26.5\ kg\ m^{-3}$ isopycnal surface, the largest trends (maximum nitrate trend of $0.11\ \mu mol\ kg^{-1}\ y^{-1}$ at Station 90.110) are in the offshore region, and weaker trends are observed within the immediate influence of the CUC, a pattern similar to the DO trends. Although there is a cross-shore difference in the magnitude of the nitrate and phosphate trends, they are increasing throughout the region over the 28-year period. These spatial patterns are consistent with influences from the dominant source waters to the region, from both mid-latitudes (Whitney et al., 2013) and the eastern tropical Pacific via transport of low-nutrient waters within the CUC (Castro et al., 2001; Meinville and Johnson, 2013).

The spatial patterns of silicic acid trends are considerably more complex than those of the other variables (Fig. 3). As with nitrate and phosphate, there are strong positive trends in silicic acid in the offshore portion of the grid at both density levels. Unique to silicic acid, however, is a strong decreasing trend within the SCB at the $\sigma_\theta=26.5\ kg\ m^{-3}$ isopycnal surface, with a maximum decline of $-0.05\ \mu mol\ kg^{-1}\ y^{-1}$ at Station 90.45. In the region of the CUC, there are strong and opposing silicic acid trends at the upper and lower-pycnocline depths. The lower positive nitrate trends, and negative silicic acid trends, near the CUC core are consistent with the transport of low-nutrient tropical waters (Meinville and Johnson, 2013). The variable spatial patterns of trends in the inorganic nutrients yield interesting patterns in the nutrient ratio trends. Trends in the N:P ratio are of opposite sign at the two levels in the offshore portion of the grid, but are strongly negative on the $\sigma_\theta=26.5\ kg\ m^{-3}$ isopycnal surface within the SCB. Trends in the Si:N ratio are also negative throughout the region, and strongest at the southern end of the grid at both levels.

3.3. Cross-shore structure of water mass variability

Time-longitude plots of spiciness and silicic acid on the $\sigma_\theta=26.5\ kg\ m^{-3}$ isopycnal surface reveal details of the cross-shore structure in lower pycnocline water mass variability in the region (Fig. 4). The spiciness diagram summarizes interannual thermohaline variability along Line 93 over the 28-year record, and reveals a cross-shore dichotomy in the frequency of variability (see also Bograd and Lynn, 2003). The high spiciness signature of El Niño events is evident in 1997–98 and 2002–04, but is generally confined to within 200 km of shore (Fig. 4A). The offshore region is characterized by longer periods of relatively lower or higher spiciness, most likely reflecting low-frequency variations in the NPSG (expansion or contraction of the Gyre), but a much lower range of variability (Bograd and Lynn, 2003). The post-2000 period has been characterized by higher subsurface spiciness values in the offshore region.

The silicic acid diagram demonstrates the strong variability in nutrient content at this level (Fig. 4B), and different trends within the SCB and offshore regions, similar to the spiciness pattern. Prior to 1995, there was a consistently strong cross-shore silicic acid

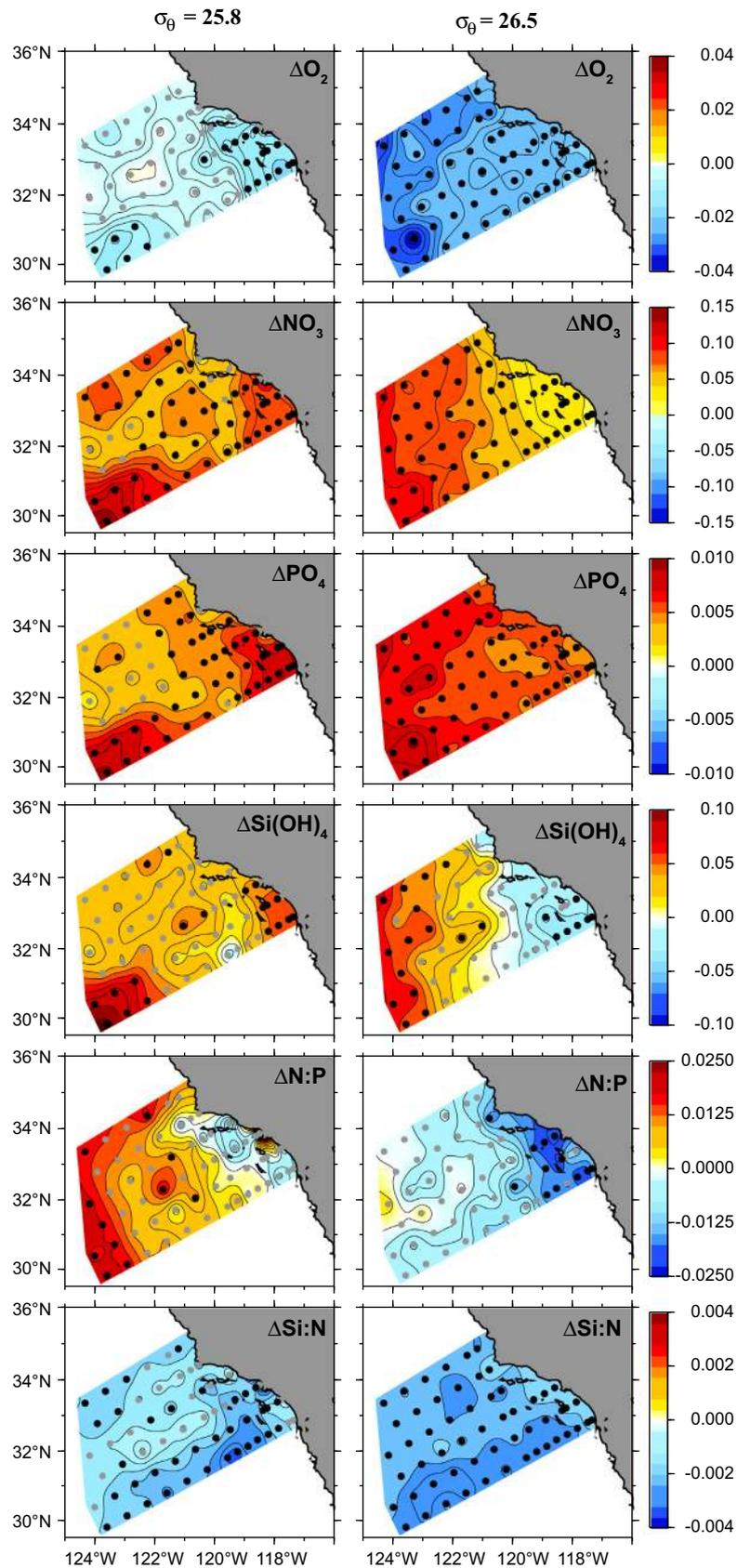


Fig. 3. Maps of linear trends in water properties over the period 1984–2012 on the $\sigma_\theta=25.8 \text{ kg m}^{-3}$ isopycnal surface (left panels) and the $\sigma_\theta=26.5 \text{ kg m}^{-3}$ isopycnal surface (right panels). From top to bottom, dissolved oxygen ($\text{mL L}^{-1} \text{ y}^{-1}$), nitrate ($\mu\text{mol kg}^{-1} \text{ y}^{-1}$), phosphate ($\mu\text{mol kg}^{-1} \text{ y}^{-1}$), silicic acid ($\mu\text{mol kg}^{-1} \text{ y}^{-1}$), nitrate:phosphate ratio (y^{-1}), and silicic acid:nitrate ratio (y^{-1}). Stations with significant linear regressions ($p < 0.001$) are shown with black dots.

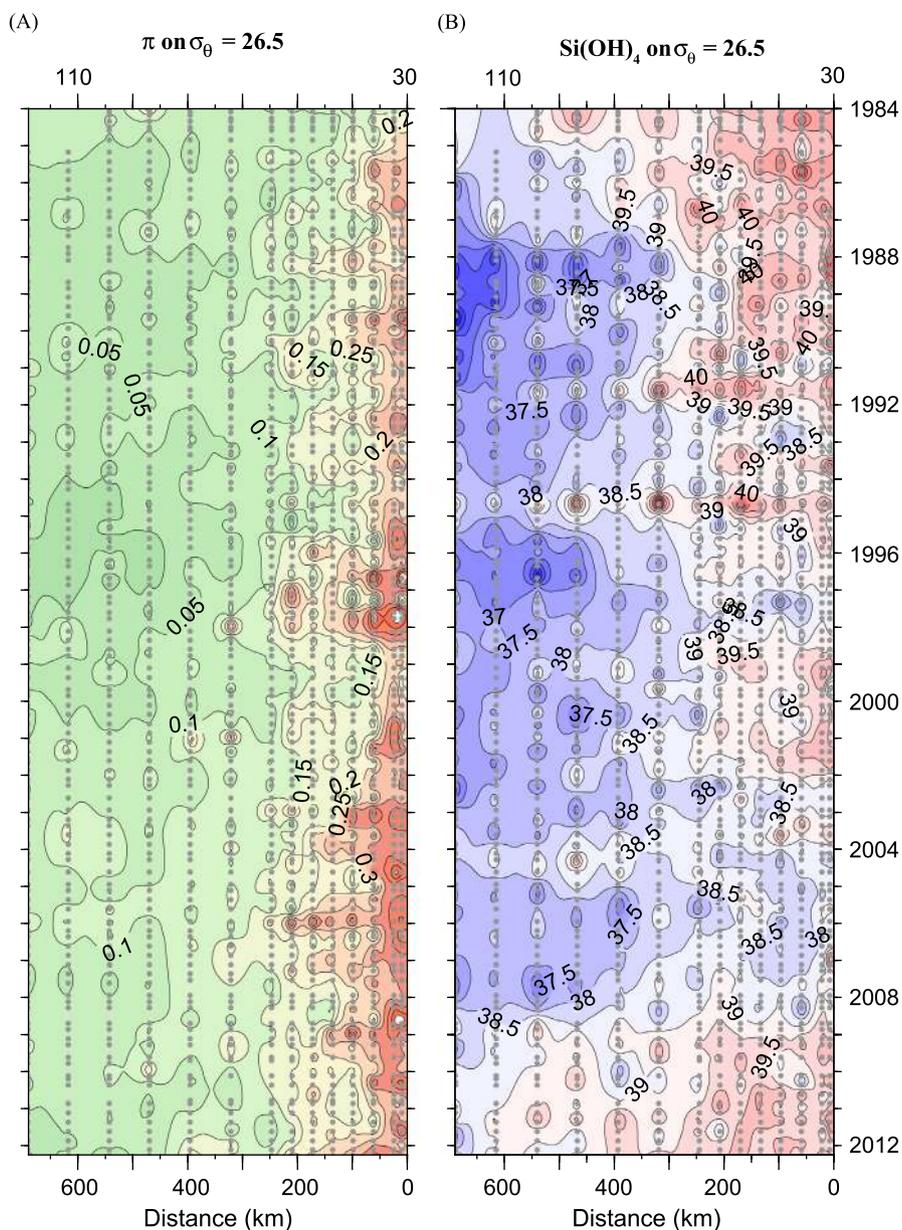


Fig. 4. Time-longitude plots, 1984–2012, of (A) spiciness (kg m^{-3}) and (B) silicic acid ($\mu\text{mol kg}^{-1}$) on the $\sigma_{\theta}=26.5 \text{ kg m}^{-3}$ isopycnal surface along a portion of CalCOFI line 93. CalCOFI station numbers are given on top axes, and all station occupations are marked with gray dots.

gradient within the lower pycnocline, with relatively high values shoreward of 300 km and lower values further offshore. The strong positive silicic acid trend offshore and weak declining trend within the SCB has led to a significantly weaker cross-shore gradient since then (see also Figs. 2 and 3).

4. Discussion and conclusions

We have used the post-1984 CalCOFI hydrographic record to quantify water mass variability throughout the CCE-LTER/CalCOFI region. Dissolved oxygen shows a strong decline at mid-depths (within the pycnocline) throughout the region; in fact, the declines described in Bograd et al. (2008) have continued over most of the region with inclusion of an additional six years of data. Concurrent with the oxygen decline are strong increases in nitrate and phosphate concentrations at both upper and mid-pycnocline depths, with spatial patterns that match those of DO. Silicic acid

also shows an increasing trend in the offshore portion of the region, consistent with oxygen and the macro-nutrients, but has strong and opposing trends in the upper (increasing) and mid-pycnocline (decreasing) depths. The varying rates of change in the inorganic nutrients yield a more complex pattern of variability in the nutrient ratios. These regional patterns, occurring at depths strongly impacted by advection, imply variability over long time and broader spatial scales, i.e., within the source waters. Indeed, trends in spiciness on Line 93 show a strong increase over the 28-year record within and at the depth of the CUC core (and declining spiciness, indicative of cooling, in the upper 100 m) (Fig. 5). This suggests that modified waters advected from the NPSG and the eastern tropical Pacific are impacting the region. Furthermore, the biogeochemical trends observed throughout the CCE-LTER region are of the same sign and magnitude to those observed in the western and eastern subarctic Pacific (Whitney et al., 2013), implying basin-scale climate forcing of oxygen and nutrient variability.

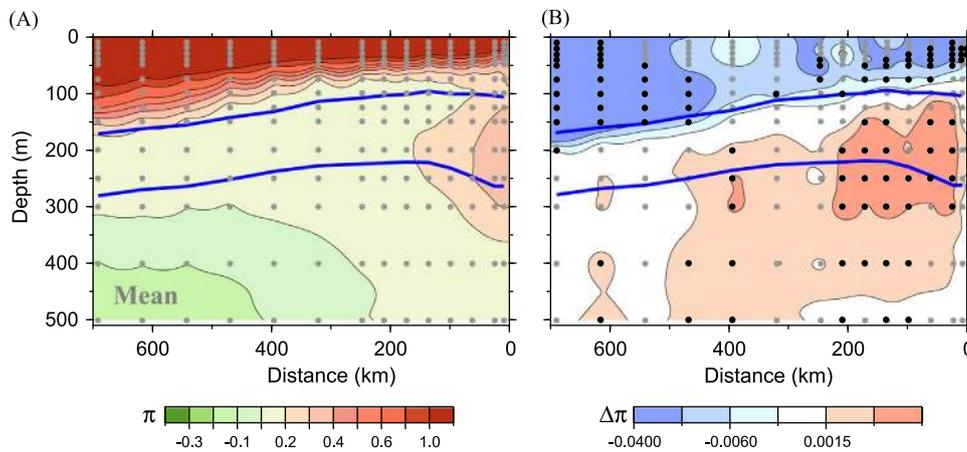


Fig. 5. (A) Mean autumn (October–November) spiciness (kg m^{-3}) and (B) linear trend in spiciness over the period 1984–2012 ($\text{kg m}^{-3} \text{y}^{-1}$) on Line 93. Mean depths of the $\sigma_{\theta}=25.8 \text{ kg m}^{-3}$ and $\sigma_{\theta}=26.5 \text{ kg m}^{-3}$ isopycnal surfaces are shown by the blue lines. Climatology is for the 1984–2012 period. The CUC core is evident as the coastal bolus of high spiciness at mid-depths. Stations/depths with significant linear regressions ($p < 0.001$) are shown with black dots in (B).

4.1. Source water changes

Global ocean reanalysis products were used to identify potential mechanisms and time scales of the observed variability in subsurface water mass properties. Using the ECMWF ORA-S3 and SODA 2.1.6 reanalysis we define an index of the temporal evolution of the monthly subsurface spiciness anomalies along the $\sigma_{\theta}=26.5 \text{ kg m}^{-3}$ isopycnal surface. This index is the spatial average of the spiciness anomalies in the region defined by the coordinates 29.73°N – 41.73°N and 129.95°W – 120.79°W (green box on Fig. 6A,B). We refer to this index as the CCS-spice index. Correlations maps of the CCS-spice index and the time series of spiciness anomalies for grid locations in the eastern Pacific along the $\sigma_{\theta}=26.5 \text{ kg m}^{-3}$ isopycnal surface show a strong agreement between SODA 2.1.6 and ORA-S3 (Fig. 6A,B). The temporal evolution of the spiciness anomalies obtained from the two reanalysis products also shows a positive trend component (Fig. 6C) between the period 1984 and 2009 that is consistent with the CalCOFI hydrography. However, if we consider the entire extent of the record, these anomalies are characterized by substantial interdecadal changes, which need further investigation when assessing the significance of the observed trends after 1984.

To understand the link between the low-frequency anomalies in the source waters and the subsurface advection dynamics we conducted a simple lead–lag correlation analysis. Fig. 7 shows a sequence of lagged correlation maps between the ORA-S3 spiciness index and the spiciness anomalies along the $\sigma_{\theta}=26.5 \text{ kg m}^{-3}$ isopycnal surface. These maps suggest that the anomalies found in the CCS region propagate downstream following the path of the mean subtropical gyre circulation. These anomalies can be identified 5 years earlier in the North Pacific drift region around 40°N (Fig. 7A) and 3 years later around 20°N (Fig. 7D). Recent studies have used Argo profiles to track the propagation of large-scale spiciness anomalies throughout the subtropical and tropical North Pacific (Sasaki et al., 2010; Li et al., 2012), with a propagation path and speed consistent with advection by the mean flow. These observations are similar to those observed here, although the Argo-derived anomalies were observed at a shallower level ($25.0 < \sigma_{\theta} < 25.5$) and propagated more quickly.

Meinvielle and Johnson (2013) also observed a positive spiciness trend in the eastern Pacific and attributed it to a northward shift of Pacific Equatorial Water transported via the CUC. This is consistent with the spatial pattern of the CalCOFI nutrient trends, which showed a clear CUC signal within the Southern California Bight (weaker positive nitrate and phosphate trends, negative

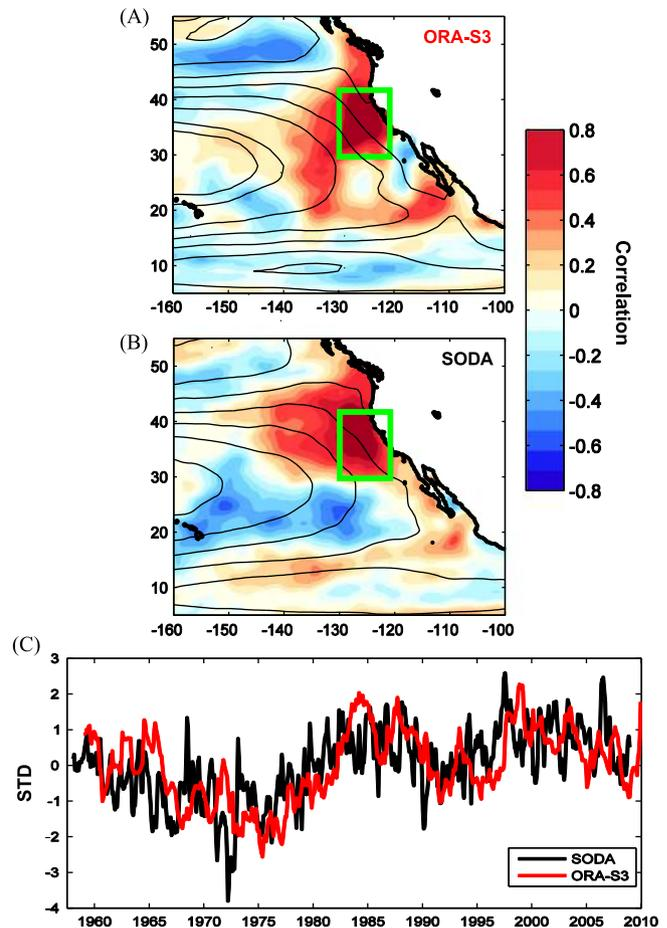


Fig. 6. Correlation between CCS-spice index (average spiciness anomaly in the region of the green box) and spiciness anomalies on the $\sigma_{\theta}=26.5 \text{ kg m}^{-3}$ isopycnal surface from the (A) ORA-S3 and (B) SODA 2.1.6 reanalysis products. Contours represent the mean streamfunction along the $\sigma_{\theta}=26.5 \text{ kg m}^{-3}$ isopycnal. (C) Time series of ORA-S3 (red) and SODA 2.1.6 (black) spiciness index over the period 1958–2010. The indices have been normalized by the standard deviation.

silicic acid trend). These results indicate that large-scale subsurface climate dynamics may have a strong impact on the water properties of the CCE-LTER region, and particularly at the depths of source waters for upwelling (Chhak and Di Lorenzo, 2007).

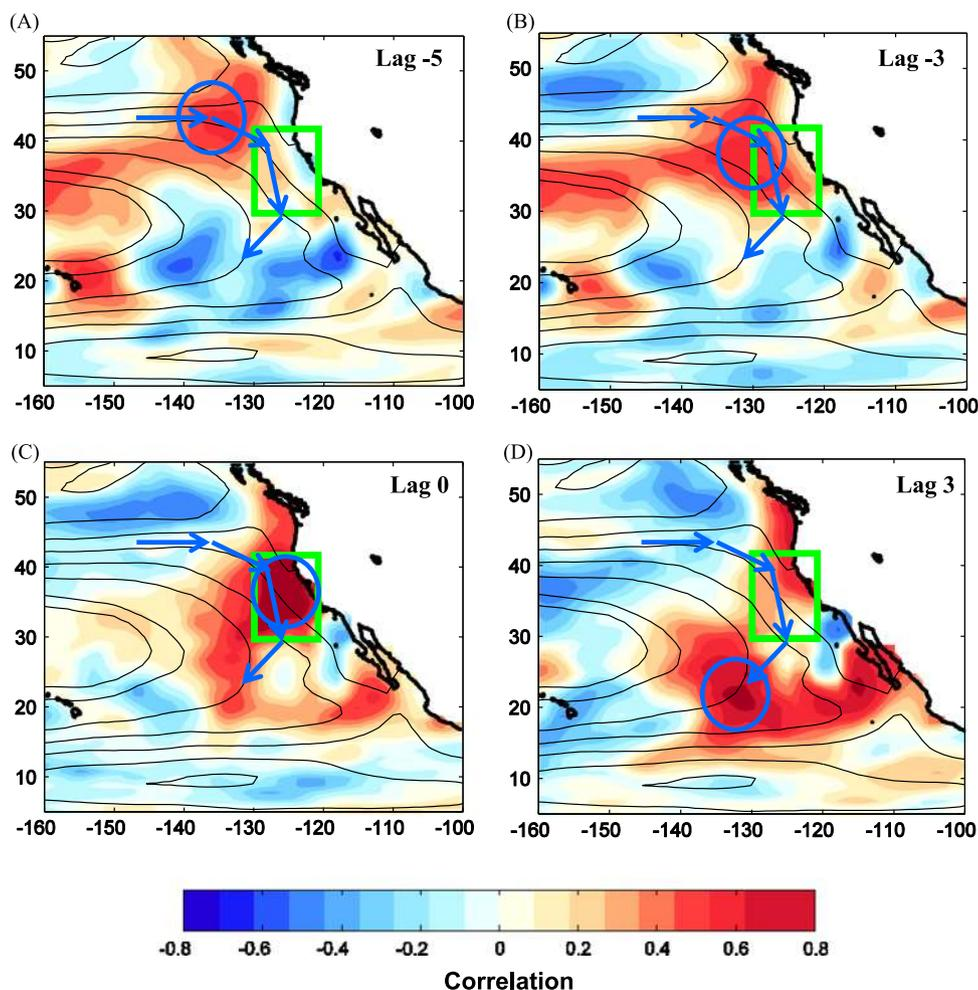


Fig. 7. Lead-lag correlation maps between the CCS-spice index and the spiciness field on the $\sigma_{\theta}=26.5 \text{ kg m}^{-3}$ isopycnal surface from the ORA-S3 reanalysis for (A) lag of 5 years, (B) lag of 3 years, (C) no lag, and (D) lead of 3 years. CCS-spice index is the average spiciness in the region of the green box. Arrows show direction of advection by the mean circulation. Contours represent the mean streamfunction along the $\sigma_{\theta}=26.5 \text{ kg m}^{-3}$ isopycnal during the period 1959–2009.

4.2. Biological implications

The water mass changes described here could have important ecosystem implications. Using a suite of satellite products to examine chlorophyll-*a* concentrations off the California coast from 1996 to 2011, Kahru et al. (2012) determined that offshore waters had significantly decreased their chlorophyll-*a* concentrations. During the same time interval, nearshore waters exhibited significantly increased chlorophyll-*a* concentrations, particularly in the SCB, consistent with the surface nutrient trends observed here.

Within the Santa Barbara Basin, a unique suite of biological time series allows an examination of the potential impacts of the observed water property changes, particularly the stoichiometric changes. Recent studies here suggest taxonomic shifts have occurred over the last decade, with more intense diatom blooms in spring and summer and fewer large dinoflagellate blooms beginning in 2001 (Anderson et al., 2008). A decrease in seasonally corrected integrated biogenic Si concentrations over the same time period, further suggests that these blooms may also signal a change in the speciation of the diatom-dominated food web that occurs during the upwelling season (Krause et al., 2013). Indeed, evidence from a deep-moored sediment trap indicates that in 2000, there was an abrupt shift towards greater frequency and abundance of the neurotoxin producing, lightly silicified diatom, *Pseudo-nitzschia*. Furthermore, these *Pseudo-nitzschia* produced more of the toxin domoic acid, with only one large event ($> 5 \text{ mg m}^{-2} \text{ d}^{-1}$) from 1993 to 1999 versus 16

large events from 2000 to 2008 (Sekula-Wood et al., 2011). Such a transition in domoic acid production is consistent with previous research that suggests domoic acid production increases under Si or P limitation in uni-algal continuous and batch culture experiments (Pan et al., 1996, 1998; Bates et al., 1998; Fehling et al., 2004). Field studies have also linked low Si:P and Si:N to the presence of toxic *Pseudo-nitzschia* blooms in both the Santa Barbara Basin (Anderson et al., 2006, 2009, 2011) and the San Pedro Basin regions of the SCB (Schnetzer et al., 2007). Thus, we hypothesize that the altered biogeochemistry of upwelled source waters from the CUC is impacting phytoplankton composition as well as the intensity and frequency of toxic *Pseudo-nitzschia* blooms.

The biogeochemical changes observed here could have broader biological impacts throughout the region, including 'upstream' where modified waters provide a source for coastal upwelling. More studies are needed to address the forcing dynamics of these source water modifications, their impact on the transformation of upwelled water masses, and their effects on regional ecosystem processes, including changes in the abundance and community structure of zooplankton and ichthyoplankton (e.g., Chhak and Di Lorenzo, 2007).

Acknowledgments

We thank Xuemei Qiu for analysis and graphics assistance. We acknowledge the quality and longevity of the CalCOFI program,

and the many scientists and seagoing staff who have contributed to the collection, processing, and analysis of this excellent data set. We also acknowledge the California Current Ecosystem Long-Term Ecosystem Research (CCE-LTER) project, supported by a grant from NSF (OCE-0417616). The comments of two anonymous reviewers improved the manuscript.

References

- Anderson, G.C., 1971. Oxygen analysis, in Marine Technician's Handbook, SIO Ref. 71-8. Scripps Inst. of Oceanogr, La Jolla, California.
- Anderson, C.R., Brzezinski, M.A., Washburn, L., Kudela, R., 2006. Circulation and environmental conditions during a toxigenic *Pseudo-nitzschia australis* bloom in the Santa Barbara Channel, California. *Mar. Ecol. Prog. Ser.* 327, 119–133.
- Anderson, C.R., Siegel, D.A., Brzezinski, M.A., Guillocheau, N., 2008. Controls on temporal patterns in phytoplankton community structure in the Santa Barbara Channel, California. *J. Geophys. Res.* 113, C04038, <http://dx.doi.org/10.1029/2007JC004321>.
- Anderson, C.R., Siegel, D.A., Kudela, R.M., Brzezinski, M.A., 2009. Empirical models of toxigenic *Pseudo-nitzschia* blooms: potential use as a remote detection tool in the Santa Barbara Channel. *Harmful Algae* 8 (3), 478–492.
- Anderson, C.R., Kudela, R.M., Benitez-Nelson, C.R., Sekula-Wood, E., Burrell, C., Langlois, G., Siegel, D., 2011. Detecting toxic diatom blooms from ocean color and a regional ocean model. *Geophys. Res. Lett.*, 38, <http://dx.doi.org/10.1029/2010GL045858>.
- Atlas, E.L., Callaway, J.C., Tomlinson, R.D., Gordon, L.L., Barstow, L., Park, P.K., 1971. A Practical Manual for Use of the Technicon AutoAnalyzer in Seawater Nutrient Analysis. Oregon State University, Corvallis, Oregon p. 215 (Technical Report).
- Balmaseda, M.A., Vidard, A., Anderson, D.L.T., 2008. The ECMWF ocean analysis system: ORA-S3. *Mon. Weather Rev.* 136 (8), 3018–3034.
- Bates, S.S., Garrison, D.L., Horner, R.A., 1998. Bloom dynamics and physiology of domoic acid producing *Pseudo-nitzschia* species. In: Anderson, D.M., Cembella, A.D., Hallegraeff, G.M. (Eds.), *Physiological Ecology of Harmful Algal Blooms*. Springer-Verlag, Heidelberg.
- Bernhardt, J.R., Leslie, H.M., 2013. Resilience to climate change in coastal marine ecosystems. *Annu. Rev. Mar. Sci.* 5, 371–392.
- Bograd, S.J., Lynn, R.J., 2001. Physical-biological coupling in the California Current during the 1997–99 El Niño – La Niña cycle. *Geophys. Res. Lett.* 28, 275–278.
- Bograd, S.J., Lynn, R.J., 2003. Long-term variability in the southern California current system. *Deep-Sea Res. II* 50 (14–16), 2355–2370.
- Bograd, S.J., Castro, C.G., Di Lorenzo, E., Palacios, D.M., Bailey, H., Gilly, W., Chavez, F. P., 2008. Oxygen declines and the shoaling of the hypoxic boundary in the California current. *Geophys. Res. Lett.* 35 (12), <http://dx.doi.org/10.1029/2008GL034185>.
- Booth, J.A.T., McPhee-Shaw, E., Chua, P., Kingsley, E., Denny, M., Phillips, R., Bograd, S.J., Zeidberg, L.D., Gilly, W.F., 2012. Natural intrusions of hypoxic, low pH water into nearshore marine environments on the California coast. *Cont. Shelf Res.* 45, 108–115.
- Burrows, M.T., Schoeman, D.S., Buckley, L.B., Moore, P., Poloczanska, E.S., Brander, K. M., Brown, C., Bruno, J.F., Duarte, C.M., Halpern, B.S., Holding, J., Kappel, C.V., Kiessling, W., O'Connor, M.I., Pandolfi, J.M., Parmesan, C., Schwing, F.B., Sydeman, W.J., Richardson, A.J., 2011. The pace of shifting climate in marine and terrestrial ecosystems. *Science*, 334, <http://dx.doi.org/10.1126/science.1210288>.
- Carton, J.A., Giese, B.S., 2008. A reanalysis of ocean climate using Simple Ocean Data Assimilation (SODA). *Mon. Weather Rev.* 136, 2999–3017.
- Carpenter, J.H., 1965. The Chesapeake Bay Institute technique for the Winkler dissolved oxygen method. *Limnol. Oceanogr.* 10, 141–143.
- Castro, C.G., Chavez, F.P., Collins, C.A., 2001. Role of the California Undercurrent in the export of denitrified waters from the eastern tropical North Pacific. *Glob. Biogeochem. Cycle* 15 (4), 819–830.
- Chan, F., Barth, J.A., Lubchenco, J., Kirincich, A., Weeks, H., Peterson, W.T., Menge, B. A., 2008. Emergence of anoxia in the California current large marine ecosystem. *Science* 319 (5865), 920.
- Chhak, K., Di Lorenzo, E., 2007. Decadal variation in the California Current upwelling cells. *Geophys. Res. Lett.* 34 (L14604).
- Chelton, D.B., 1984. Seasonal variability of alongshore geostrophic velocity off central California. *J. Geophys. Res.* 89, 3473–3486.
- Deutsch, C., Emerson, S., Thompson, L., 2005. Fingerprints of climate change in North Pacific oxygen. *Geophys. Res. Lett.*, 32, <http://dx.doi.org/10.1029/2005GL023190>.
- Deutsch, C., Brix, H., Ito, T., Frenzel, H., Thompson, L., 2011. Climate-forced variability of ocean hypoxia. *Science*, 333, <http://dx.doi.org/10.1126/science.1202422>.
- Di Lorenzo, E., Fiechter, J., Schneider, N., Bracco, A., Miller, A.J., Franks, P.J.S., Bograd, S.J., Moore, A.M., Thomas, A.C., Crawford, W.J., Peña, A., Hermann, A., 2009. Nutrient and salinity decadal variations in the central and eastern North Pacific. *Geophys. Res. Lett.* 36, L14601, <http://dx.doi.org/10.1029/2009GL038261>.
- Doney, S.C., Fabry, V.J., Feely, R.A., Kleypas, J.A., 2009. Ocean acidification: the other CO₂ problem. *Annu. Rev. Mar. Sci.* 1, 169–192.
- Doney, S.C., Ruckelshaus, M., Duffy, J.E., Barry, J.P., Chan, F., et al., 2012. Climate change impacts on marine ecosystems. *Annu. Rev. Mar. Sci.* 4, 11–37.
- Fehling, J., Davidson, K., Bolch, C.J., Bates, S.S., 2004. Growth and domoic acid production by *Pseudo-nitzschia seriata* (Bacillariophyceae) under phosphate and silicate limitation. *Phycologia* 40 (4), 674–683.
- Flament, P., 2002. A state variable for characterizing water masses and their diffusive stability: spiciness. *Prog. Oceanogr.* 54, 493–501.
- Freeland, H.J., Denman, K.L., Wong, C.S., Whitney, F., Jacques, R., 1997. Evidence of change in the winter mixed layer in the Northeast Pacific Ocean. *Deep-Sea Res.* 44, 2117–2129.
- Garcia, H., Gordon, L., 1992. Oxygen solubility in seawater: better fitting equations. *Limnol. Oceanogr.* 37, 1307–1312.
- Gordon, L.L., Jennings, J.C., Ross, A.A., Krest, J.M., 1993. A suggested protocol for continuous flow automated analysis of seawater nutrients (phosphate, nitrate, nitrite and silicic acid) in the WOCE Hydrographic Program and the Joint Global Ocean Flux Study. WOCE Operations Manual, Part 3.1.3, WHP Office Report WHP0 91-1.
- Gruber, N., 2011. Warming up, turning sour losing breath: ocean biogeochemistry under global change. *Philos. Trans. R. Soc. A* 369 (1943), <http://dx.doi.org/10.1098/rsta.2011.0003>.
- Gruber, N., Hauri, C., Lachkar, Z., Loher, D., Frolicher, T.L., Plattner, G.-K., 2012. Rapid progression of ocean acidification in the California Current. *Science*, <http://dx.doi.org/10.1126/science.1216773>.
- Hauri, C., Gruber, N., Plattner, G.-K., Alin, S., Feely, R.A., Hales, B., Wheeler, P.A., 2009. Ocean acidification in the California Current System. *Oceanography* 22 (4), 60–71.
- Hewitt, R.P., 1988. Historical review of the oceanographic approach to fishery research. *CalCOFI Rep.* 29, 27–41.
- Hickey, B.M., 1979. The California current system – hypotheses and facts. *Prog. Oceanogr.* 8, 191–279.
- Hickey, B.A., 1998. Western North America, tip of Baja California to Vancouver Island. In: Brink, K., Robinson, A. (Eds.), *The Sea*, 11. Wiley, New York, pp. 345–394.
- Kahru, M., Kudela, R.M., Manzano-Sarabia, M., Mitchell, B.G., 2012. Trends in the surface chlorophyll of the California Current: merging data from multiple ocean color satellites. *Deep-Sea Res. II* 77, 89–98.
- Karl, D.M., Church, M.J., Dore, J.E., Letelier, R.M., Mahaffey, C., 2012. Predictable and efficient carbon sequestration in the North Pacific Ocean supported by symbiotic nitrogen fixation. *Proc. Nat. Acad. Sci. USA* 109, 1842–1849.
- Keeling, R.F., Garcia, H.E., 2002. The change in oceanic O₂ inventory associated with recent global warming. *Proc. Nat. Acad. Sci. USA* 99, 7848–7853.
- Keeling, R.F., Kortzinger, A., Gruber, N., 2010. Ocean deoxygenation in a warming world. *Annu. Rev. Mar. Sci.* 2, 199–229.
- Koslow, J.A., Goericke, R., Lara-Lopez, A., Watson, W., 2011. Impact of declining intermediate-water oxygen on deepwater fishes in the California Current. *Mar. Ecol. Prog. Ser.* 436, 207–218.
- Krause, J.W., Brzezinski, M.A., Siegel, D.A., Thunell, R.C., 2013. Biogenic silica standing stock and export in the Santa Barbara Channel ecosystem. *J. Geophys. Res.* 118, 1–14, <http://dx.doi.org/10.1029/2012JC008070>.
- Li, Y., Wang, F., Sun, Y., 2012. Low-frequency spiciness variations in the tropical Pacific Ocean observed during 2003–2012. *Geophys. Res. Lett.* 39, L23601, <http://dx.doi.org/10.1029/2012GL053971>.
- Lynn, R.J., Simpson, J.J., 1987. The California current system: the seasonal variability of its seasonal characteristics. *J. Geophys. Res.* 92 (C12), 12,947–12,966.
- Lynn, R.J., Simpson, J.J., 1990. The flow of the Undercurrent over the continental borderland off southern California. *J. Geophys. Res.* 95 (C8), 12,995–13,008.
- Lynn, R.J., Bograd, S.J., 2002. Dynamic evolution of the 1997–1998 El Niño – La Niña cycle in the southern California Current System. *Prog. Oceanogr.* 54, 59–75.
- Lynn, R.J., Bliss, K.A., Eber, L.E., 1982. Vertical and horizontal distributions of seasonal mean temperature, salinity, sigma-t, stability, dynamic height, oxygen, and oxygen saturation in the California Current, 1950–1978. *CalCOFI Atlas* no. 30, 513 pp.
- Lynn, R.J., Bograd, S.J., Chereskin, T.K., Huyer, A., 2003. Seasonal renewal of the California current: the spring transition off California. *J. Geophys. Res.*, 108, <http://dx.doi.org/10.1029/2003JC001787>.
- Mantyla, A.W., Bograd, S.J., Venrick, E.L., 2008. Patterns and controls of chlorophyll-a and primary production cycles in the Southern California Bight. *J. Mar. Syst.* 73, 48–60.
- Margalef, R., 1962. Succession in marine populations. *Adv. Front. Plant Sci.* 2, 137–188.
- Margalef, R., 1978. Life-forms of phytoplankton as survival alternatives in an unstable environment. *Oceanol. Acta* 1, 493–509.
- McClatchie, S., Goericke, R., Cosgrove, R., Auad, G., Vetter, R., 2010. Oxygen in the Southern California Bight: multidecadal trends and implications for demersal fisheries. *Geophys. Res. Lett.* 37 (19), <http://dx.doi.org/10.1029/2010GL044497>.
- Meinvielle, M., Johnson, G.C., 2013. Decadal water-property trends in the California Undercurrent, with implications for ocean acidification. *J. Geophys. Res.*, 118, <http://dx.doi.org/10.1002/2013JC009299>.
- Ono, T., Shiomoto, A., Saino, T., 2008. Recent decrease of summer nutrients concentrations and future possible shrinkage of the subarctic North Pacific high-nutrient low-chlorophyll region. *Glob. Biogeochem. Cycles* 22, GB3027, <http://dx.doi.org/10.1029/2007GB003092>.
- Ono, T., Midorikawa, T., Watanabe, Y.W., Tadokoro, K., Saino, T., 2001. Temporal increase of phosphate and apparent oxygen utilization in the subsurface waters of the western subarctic Pacific from 1968 to 1998. *Geophys. Res. Lett.* 28, 3285–3288.
- Pan, Y., Subba Rao, D.V., Mann, K.H., Brown, R.G., Pocklington, R., 1996. Effects of silicate limitation on production of domoic acid, a neurotoxin, by the diatom

- Pseudonitzschia multiseriata*. I. Batch culture studies. Mar. Ecol. Prog. Ser. 131, 225–233.
- Pan, Y., Bates, S.S., Cembella, A.D., 1998. Environmental stress and domoic acid production by *Pseudo-nitzschia*: a physiological perspective. Nat. Toxins 6, 127–135.
- Peña, M.A., Bograd, S.J., 2007. Time series of the northeast Pacific. Prog. Oceanogr. 75 (2), 115–119.
- Pierce, S.D., Smith, R.L., Kosro, P.M., Barth, J.A., Wilson, C.D., 2000. Continuity of the poleward undercurrent along the eastern boundary of the mid-latitude North Pacific. Deep-Sea Res. II 47, 811–829.
- Poloczanska, E.S., Brown, C.J., Sydeman, W.J., Kiessling, W., Schoeman, D.S., Moore, P.J., Brander, K., Bruno, J.F., Buckley, L.B., Burrows, M.T., Duarte, C.M., Halpern, B. S., Holding, J., Kappel, C.V., O'Connor, M.I., Pandolfi, J.M., Parmesan, C., Schwing, F., Thompson, S.A., Richardson, A.J., 2013. Global imprint of climate change on marine life. Nat. Clim. Chan. , <http://dx.doi.org/10.1038/nclimate1958>.
- Reid Jr., J.L., 1962. Measurements of the California Countercurrent at a depth of 250 m. J. Mar. Res. 20, 134–137.
- Reid Jr., J.L., 1963. Measurements of the California Countercurrent off Baja California. J. Geophys. Res. 68, 4819–4822.
- Sarmiento, J.L., Hughes, T.M.C., Stouffer, R.J., Manabe, S., 1998. Simulated response of the ocean carbon cycle to anthropogenic climate warming. Nature 427, 56–60.
- Sasaki, Y.N., Schneider, N., Maximenko, N., Lebedev, K., 2010. Observational evidence for propagation of decadal spiciness anomalies in the North Pacific. Geophys. Res. Lett. 37, L07708, <http://dx.doi.org/10.1029/2010GL042716>.
- Schneider, N., 2000. Decadal spiciness mode in the tropics. Geophys. Res. Lett. 27, 257–260, <http://dx.doi.org/10.1029/1999GL002348>.
- Schnetzer, A., Miller, P.E., Schaffner, R.A., Stauffer, B.A., Jones, B.H., Weisberg, S.B., DiGiacomo, P.M., Berelson, W.M., Caron, D.A., 2007. Blooms of *Pseudo-nitzschia* and domoic acid in the San Pedro Channel and Los Angeles harbor areas of the Southern California Bight, 2003–2004. Harmful Algae 6 (3), 372–387.
- Scripps Institution of Oceanography (SIO), 2012. Data Report, CalCOFI cruise 1110. CC Ref. 12-05, La Jolla, CA, 59 pp.
- Sekula-Wood, E., Benitez-Nelson, C., Morton, S., Anderson, C.R., Burrell, C., Thunell, R.C., 2011. *Pseudo-nitzschia* and domoic acid fluxes in Santa Barbara Basin (CA) from 1993 to 2008. Harmful Algae 10, 567–575.
- Simpson, J.J., Lynn, R.J., 1990. A mesoscale eddy dipole in the offshore California Current. J. Geophys. Res. 95, 13009–13022.
- Smayda, T.J., 1963. Succession of phytoplankton, and the ocean as an holocoenotic environment. In: Oppenheimer, C.H. (Ed.), Proceedings of the Symposium on Marine Microbiology. Thomas, Springfield, Illinois, pp. 260–274.
- Smith, R.D., Dukowicz, J.K., Malone, R.C., 1992. Parallel ocean general circulation modeling. Physica D 60, 38–61.
- Stewart, J.S., Hazen, E.L., Foley, D.G., Bograd, S.J., Gilly, W.F., 2012. Marine predator migration during range expansion: Humboldt squid (*Dosidicus gigas*) in the northern California Current System. Mar. Ecol. Prog. Ser. 471, 135–150.
- Stramma, L., Johnson, G.C., Sprintall, J., Mohrholz, V., 2008. Expanding oxygen-minimum zones in the tropical oceans. Science 320, 655–658.
- Stramma, L., Schmidtko, S., Levin, L.A., Johnson, G.C., 2010. Ocean oxygen minima expansions and their biological impacts. Deep-Sea Res. I 57, 1–9.
- Taylor, G.T., Muller-Karger, F., Thunell, R.C., Scranton, M.I., Astor, Y., Varela, R., Troccoli-Ghinaglia, L., Lorenzoni, L., Fanning, K.A., Hameed, S., Doherty, O., 2012. Ecosystem response to global climate change in the southern Caribbean Sea. Proc. Nat. Acad. Sci. USA. 109 (47), 19315–19320.
- Watanabe, Y.W., Shigemitsu, M., Tadokoro, K., 2008. Evidence of a change in oceanic fixed nitrogen with decadal climate change in the North Pacific subpolar region. Geophys. Res. Lett. 35, L01602, <http://dx.doi.org/10.1029/2007GL032188>.
- Whitney, F.A., 2011. Nutrient variability in the mixed layer of the subarctic Pacific Ocean, 1987–2010. J. Oceanogr. , <http://dx.doi.org/10.1007/s10872-011-0051-2>.
- Whitney, F.A., Freeland, H.J., Robert, M., 2007. Persistently declining oxygen levels in the interior waters of the eastern subarctic Pacific. Prog. Oceanogr. 75, 179–199.
- Whitney, F.A., Bograd, S.J., Ono, T., 2013. Nutrient enrichment of the subarctic Pacific Ocean pycnocline. Geophys. Res. Lett., 40, <http://dx.doi.org/10.1002/gri.50439>.
- Wolff, J., Maier-Reimer, E., Legutke, S., 1997. The Hamburg Primitive Equation Model HOPE. Technical Report 18, German Climate Computer Center (DKRZ).
- Wooster, W.S., Jones, J.H., 1970. California Undercurrent off northern Baja California. J. Mar. Res. 28, 235–250.
- Wooster, W.S., Reid Jr., J.L., 1963. Eastern boundary currents. In: Hill, M.N. (Ed.), The Sea, 1. Wiley Interscience, New York, pp. 253–280.